



Centre National d'Etudes
Spatiales



SAP_RAD_09
TRO-33-NT-2818-CNES

**Activity : CAL/VAL
SAPHIR
Side Lobe Correction**

**Prepared by : C Malassingne
(EADS-Astrium for CNES)
Verified by : A Rosak - N Karouche**

Contents

1. OBJECTIVE	2
2. OBSERVATIONS : BRIGNESS TEMPERATURE GRADIENTS	3
2.1. BRIGHTNESS TEMPERATURE GRADIENTS	3
2.2. EXAMPLE OF GRADIENTS MAPS	5
3. METHODS	7
3.1. OVERVIEW	7
4. ANTENNA PATTERN	7
4.1. COMPUTATION OF SIDE LOBES CONTRIBUTION	8
5. SUCCESS CRITERIA	9
6. PRODUCTS USED	9
7. RESULTS	9
7.1. ANALYSIS OVER 10 ORBITS	9
7.1.1. CORRECTION DISTRIBUTION OVER THE SWATH FOR THE 6 CHANNELS	9
7.1.2. CORRECTION	10
7.2. ANALYSIS OVER 14 ORBITS	11
7.2.1. CORRECTION	12
8. CONCLUSION	14

1. OBJECTIVE

Side-lobe contamination corrections are generally proposed on low frequency band radiometers, having channels that are sensing both the atmosphere and the earth surface. In those frequency bandwidths, strong brightness temperature gradients are observed mainly at Sea / Land transitions, due to difference in surface emissivity. Over these transitions, antenna side lobes contribution may affect the actual measurement of a dedicated pixel, and corrections should be implemented to cancel for the pollution coming from surrounding pixels.

Depending of the performances of the antenna in terms of side lobe levels compared to main lobe, some correction algorithm may be required

On some missions based on Nadir low frequency band radiometers, side lobe corrections tables using seasonal maps have been applied. This requires observation of the earth over long periods during first months in orbit, to define suitable correction maps with a good level of reliability and some knowledge of the signal variability as a function of time and location.

Due to the fact that the sounder is observing mainly the atmosphere, scenes with high temporal and spatial variability, at 183GHz, the above method based on a priori estimation of brightness temperature seems very complex to implement and consequently was not considered for SAPHIR.

Nevertheless, SAPHIR being a cross track radiometer, some correction algorithm using measured brightness temperature of surrounding pixels and antenna pattern derived from on ground measurement can be envisaged.

Some preliminary analysis, using a first order side lobe correction algorithm based on the brightness temperatures of the nearest surrounding pixels, and taking into account antenna efficiency, have been conducted to give some estimated figures for the impact of this possible pollution.

Finally, this technical note aims at checking if a side lobe correction algorithm is necessary for SAPHIR instrument.

2. OBSERVATIONS: BRIGHTNESS TEMPERATURE GRADIENTS

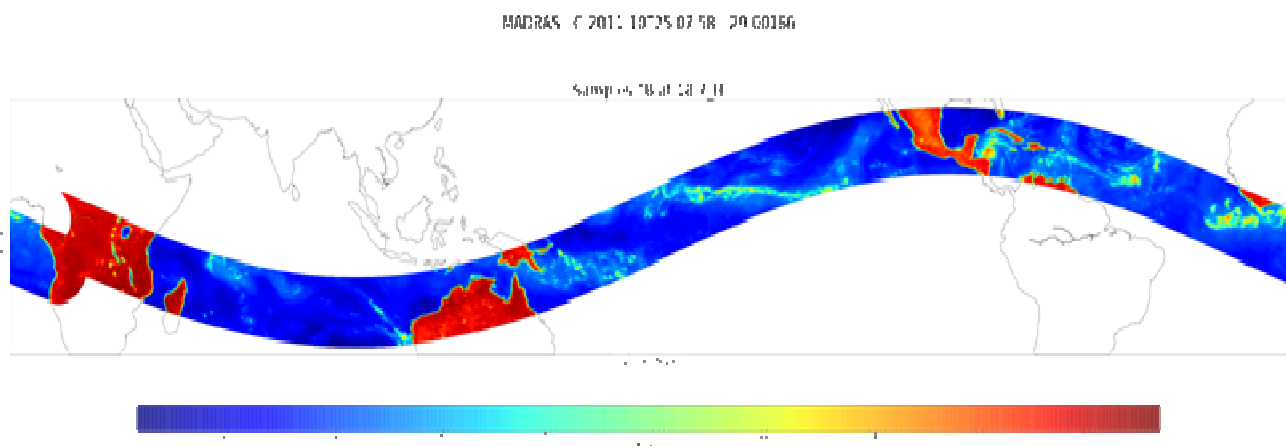
Brightness temperature gradients have been analysed using MADRAS and SAPHIR L1A data.

In those L1A products, brightness temperature is computed from the gain and the raw counts and no side lobe correction has been implemented.

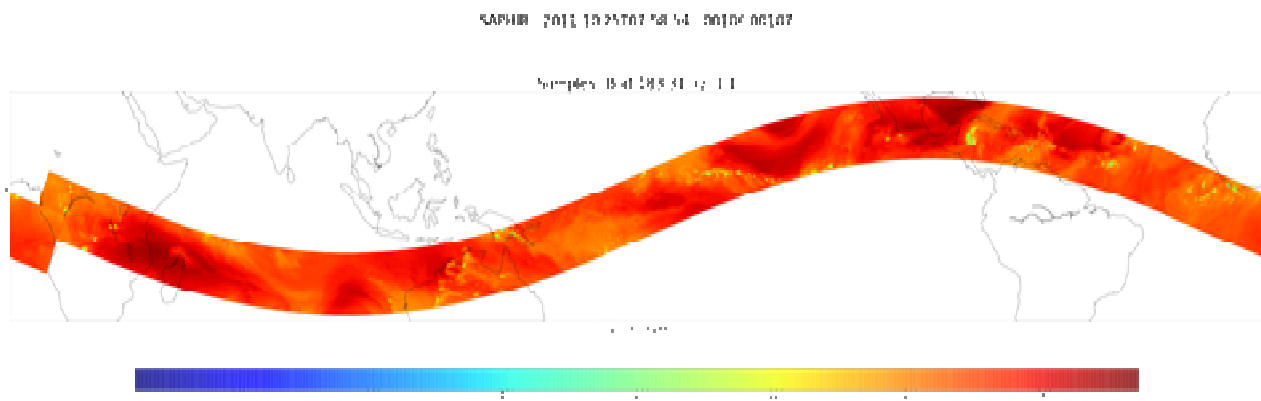
2.1. BRIGHTNESS TEMPERATURE GRADIENTS

Strong gradients are observed on low frequency band channels of MADRAS radiometer typically on the 18.7GHz H channel, embarked on the same MEGHA-TROPIQUES platform. Those gradients are mainly located over land/sea transitions.

Typical gradient values of 100 to 150K are noted on this MADRAS channel as illustrated by the following graph.



For higher frequencies (as 157GHz channel of MADRAS or 183GHz channels for SAPHIR), sensors are measuring mainly the emission of the atmosphere and not the emission from the surface. However, on Saphir Channel 6, some surface contribution can be observed. At these frequencies, the observed scenes present also a high variability, but with more limited gradients. On Saphir, typically, brightness temperatures are varying over a range of 40 to 50K if 95 % of pixels of the scene are considered.



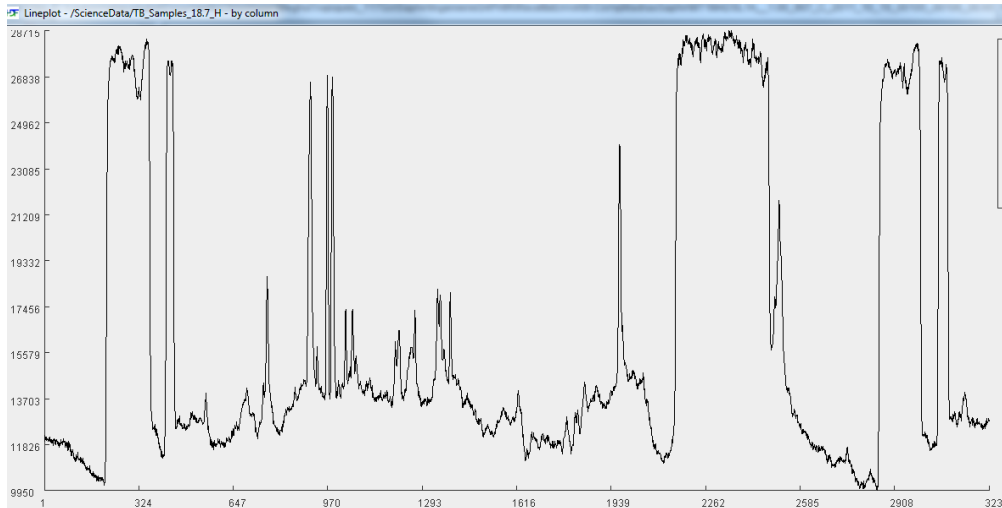
Nevertheless, locally, some significant gradients up to 150K can be observed on SAPHIR channels due to very cold clouds

The following graphs show the TB variation over one scan for both 18.7GHz and 23.8GHz Madras channels and 183.3+/-11GHz Saphir channel. In addition, min/max brightness temperature values measured on the complete set of TB data of the orbit file is provided.

Madras 18.7GHz : Orbit N°106

TB min over the orbit: 99K ;

TB max over the orbit : 292K

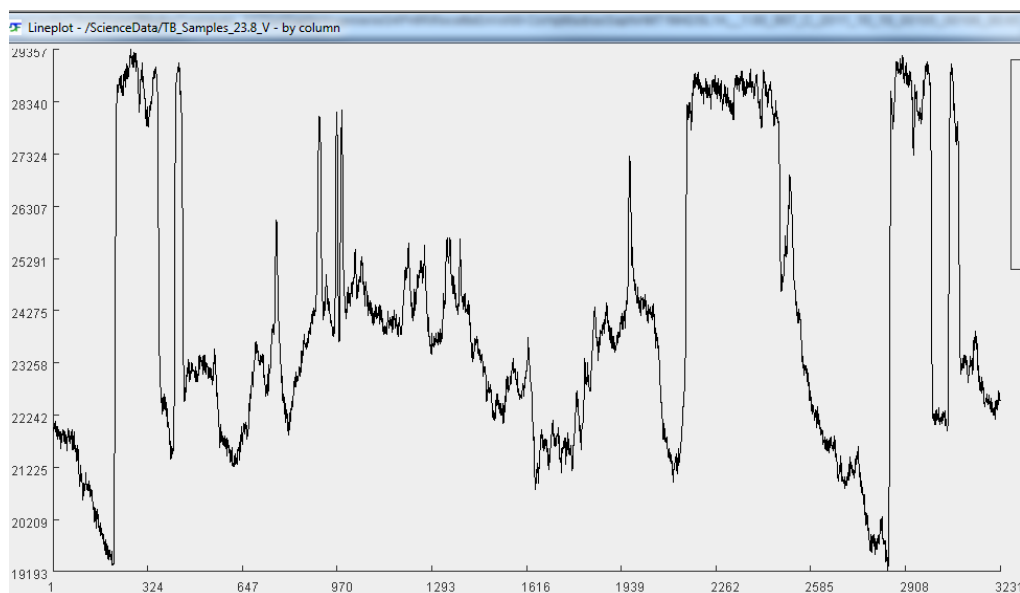


TB over one scan

Madras 23.8GHz : Orbit N° 106 :

TB min over the orbit is 188K ;

TB max over the orbit is 300K

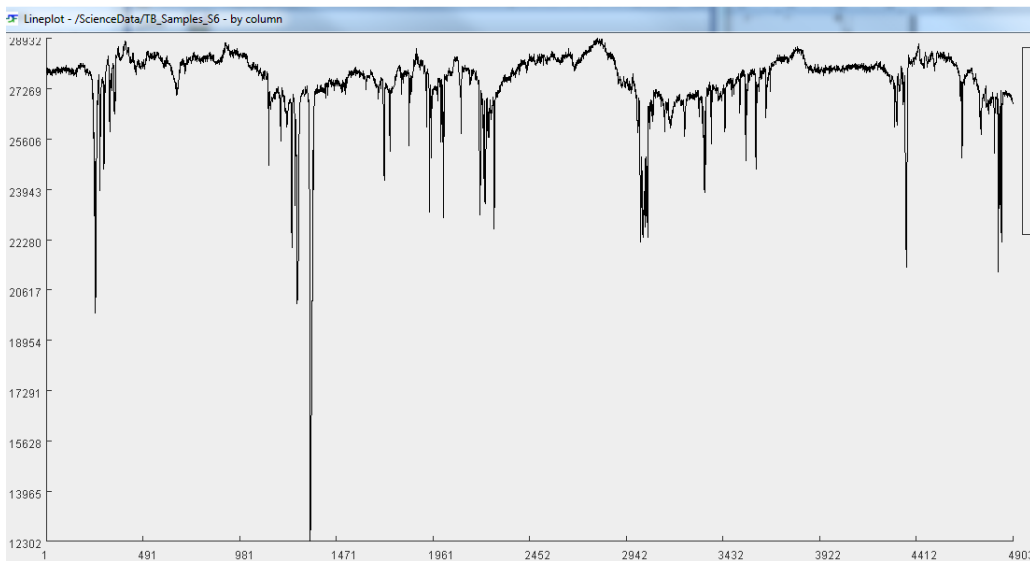


Tb over one scan

Saphir C6 channel : Orbit N°106

TB min over the orbit : 115K ;

TB max over the orbit : 294K



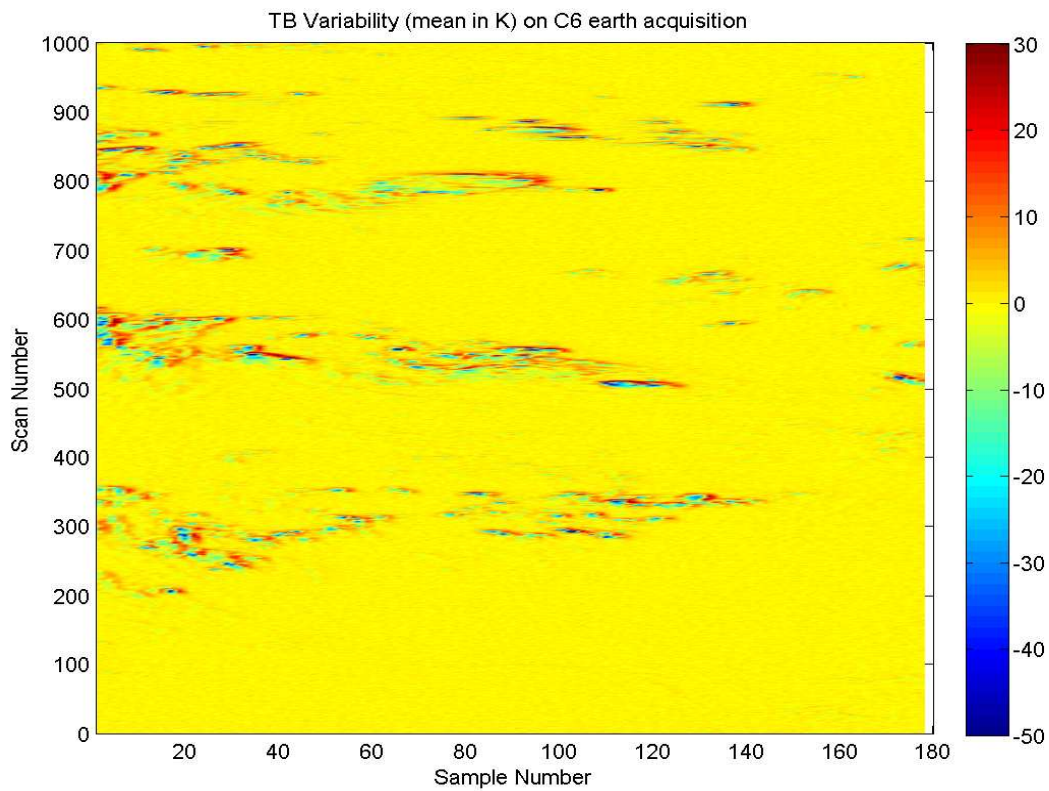
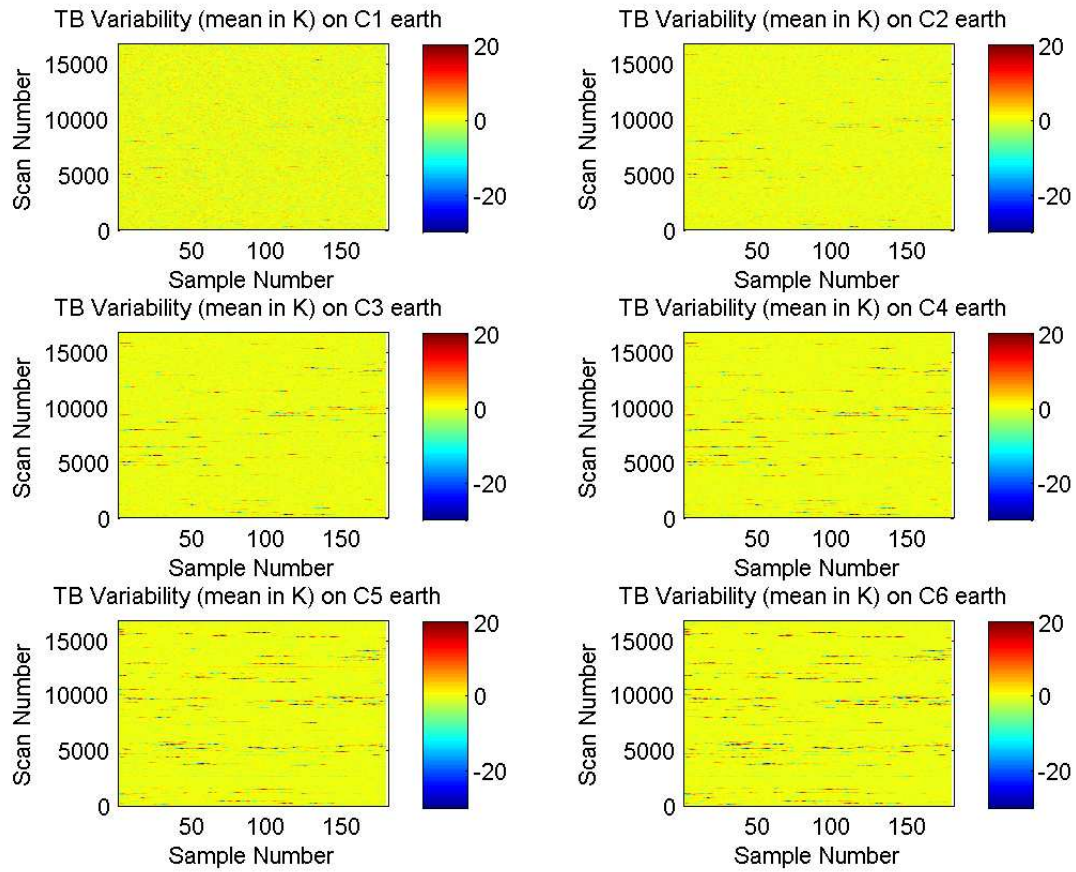
TB over one scan

Remark: On this SAPHIR scan, locally some very low brightness temperatures corresponding to some cold clouds are observed.

Finally, even if high gradients are less frequent on SAPHIR channels, we can conclude that locally, some large variations between adjacent samples can be measured.

2.2. EXAMPLE OF GRADIENTS MAPS

Gradient variations over one scene have been plotted for each channel. Each point of a plot represents the difference in Kelvin, between the measured TB sample and the averaged value of its 8 nearest neighbours. With these figures, we also confirm that strong gradient can be measured between a sample and its close environment, either with Earth surface contribution (on channel 6) or with atmosphere contribution only. Gradients are more significant for channels 5 and 6 compared to channels 3 and 4 and more significant for channel 3 and 4 compared to 1 and 2.



Zoom over Channel

3. METHODS

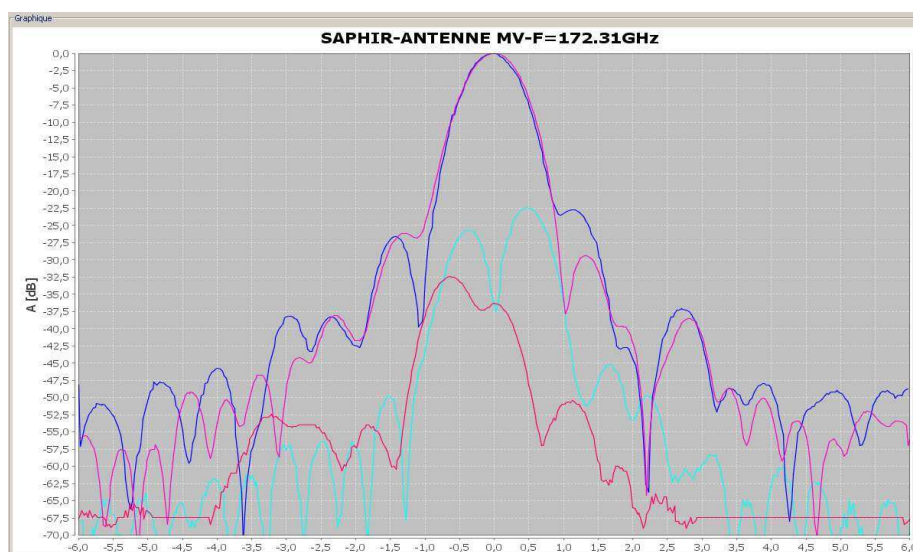
3.1. OVERVIEW

The purpose of the analysis is to estimate the impact on brightness temperature of side lobe contribution.

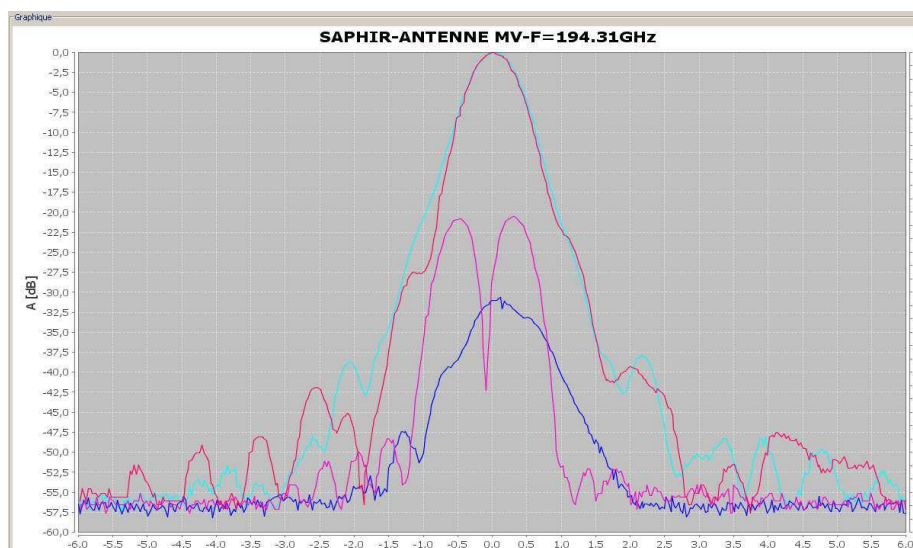
Several L1A products are cumulated over a 10 (then 14) orbits period for the analysis.

4. ANTENNA PATTERN

The antenna patterns measured on the instrument are plotted for the lowest, highest and central frequencies.

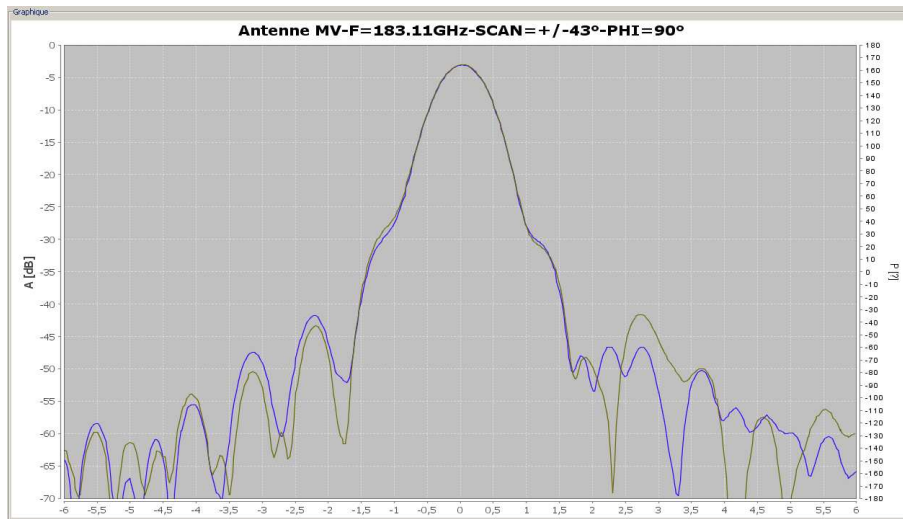


— E_{θ} , $\varphi=90^{\circ}$; — E_{θ} , $\varphi=0^{\circ}$; — E_{φ} , $\varphi=0^{\circ}$; — E_{φ} , $\varphi=90^{\circ}$



— E_{θ} , $\varphi=90^{\circ}$; — E_{θ} , $\varphi=0^{\circ}$; — E_{φ} , $\varphi=0^{\circ}$; — E_{φ} , $\varphi=90^{\circ}$

The graph hereunder show the antenna pattern measured for both extreme values of the swath, i.e. at scan angles = $\pm 43^\circ$. These values are not normalized to the maximum and show a deviation of about 3dB due to the polarization configuration of the feed of the antenna test range.



The above measurements show that, side lobes levels are less than -25dB.

The beam efficiency has been measured for each channel during the Antenna test campaign. It is defined as the ratio between integrated power in the main beam (at $2.5 \times \theta_{3dB}$) to the total power received by the antenna.

Channel	C1	C2	C3	C4	C5	C6
η_{eff} (%)	96.5	96.5	96.5	96.5	96.0	96.0

4.1. COMPUTATION OF SIDE LOBES CONTRIBUTION

A very simple method is used to give an estimation of the side lobe impact on the brightness temperature of the Earth samples.

It consists in averaging the brightness temperature of the nearest samples and correcting this value from the measured value:

$$TA = \eta_{\text{eff}} \times TB + T_{\text{sl}}$$

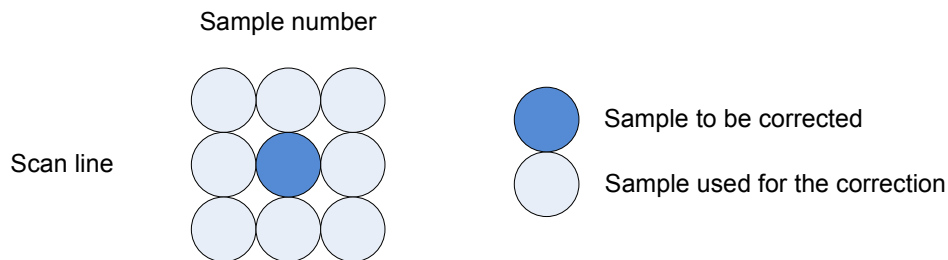
With : TA the measured antenna temperature

TB the brightness temperature

T_{sl} the secondary lobes contribution is coming from the Earth (the most important contribution) but also from the sun (direct effect and sun glint), from the sky and from the satellite itself

In our analysis, only contribution from the scene is considered. T_{sl} is computed from both in-orbit measurements (brightness temperature of the nearest samples) and on-ground measurements (beam efficiency).

Samples used for the side lobe correction:



For this analysis, it is admitted that these samples are representative of the brightness temperature “seen” by the antenna side-lobe.

The mean TB value of the 8 surrounding pixels (TB_{mean}) is computed and

$$T_{sl} = (1 - \eta_{eff}) \times TB_{mean}$$

5. SUCCESS CRITERIA

Estimate of side lobe correction contribution on SAPHIR TB is computed. Measured Antenna efficiency being quite high, this analysis should demonstrate that side lobe contribution on TB is quite limited. Nevertheless, need for correction, in L1A processing will be addressed.

6. PRODUCTS USED

A set of 10 orbits L1A data was selected for the analysis. This selected period is centred on the 4th of July 2012.

7. RESULTS

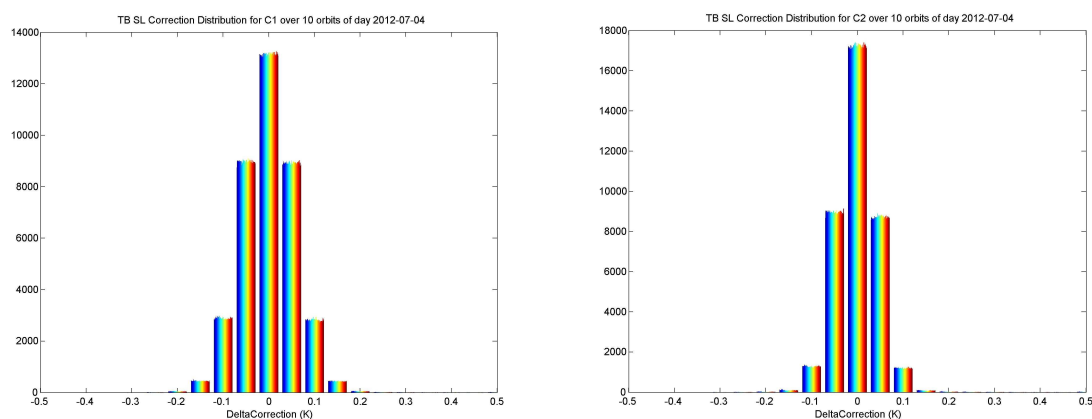
Results are presented hereafter for the six SAPHIR channels.

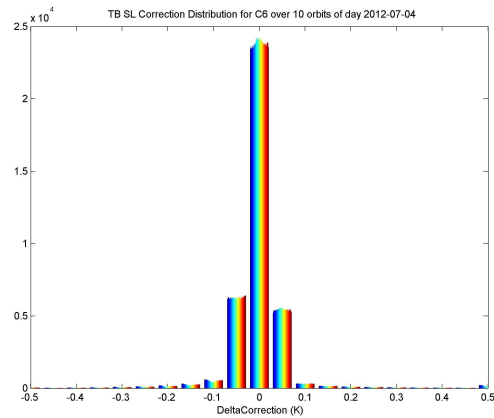
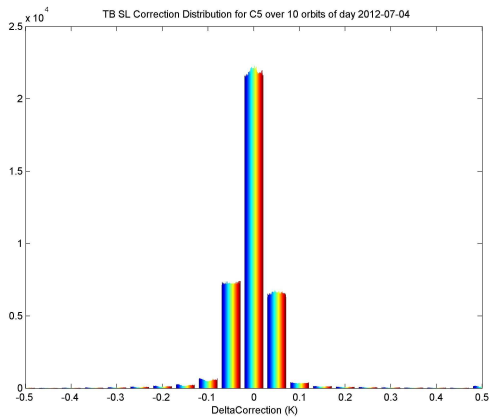
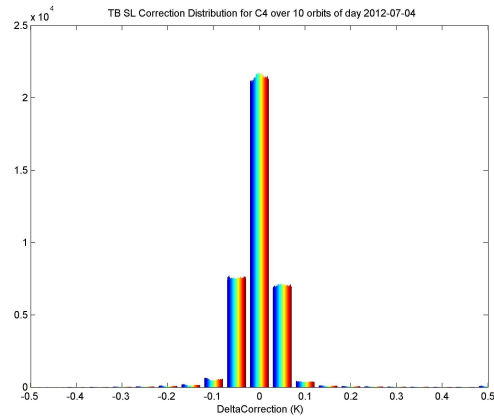
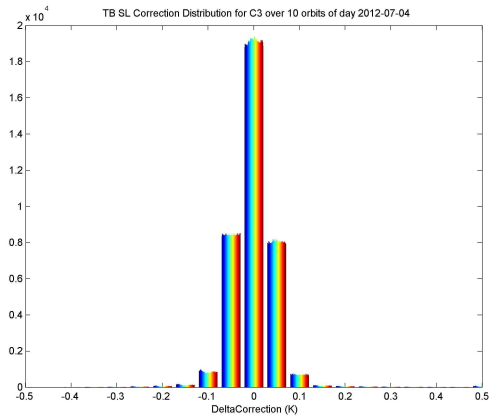
7.1. ANALYSIS OVER 10 ORBITS

The first analysis over the 10 orbits of the same day is shown for all the six channels on following graphs. 37330 scan cycles of 182 samples were processed for this analysis

7.1.1. CORRECTION DISTRIBUTION OVER THE SWATH FOR THE 6 CHANNELS

The distribution of the values of the “side lobe correction” is plotted for the six channels.





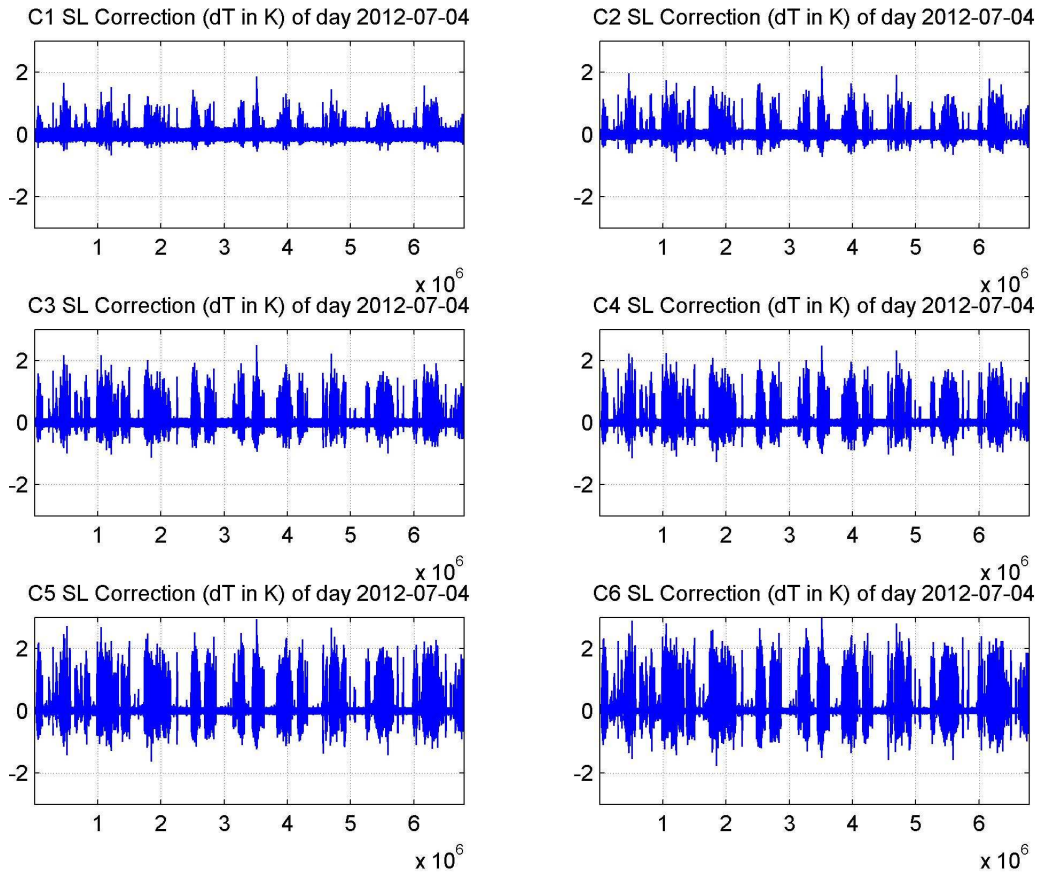
Most of the values are lower than 0.2K. There are no distribution dependence over the swath.

Remark : Colors represents sample position within the swath.

7.1.2. CORRECTION

The following graphs show the variation of the side lobe correction value in a linear representation. The 10 orbits used for this analysis results in $10 \times 3733 \times 182 = 6794060$ samples.

These graphs show that the variations of the side lobe impact follow some temporal cycles which affect all channels. The impact is lower on the channels close to 183.3GHz central frequency.



The following table summarises the degree of correction to apply due to the side-lobe contamination.

Number of samples	C1		C2		C3		C4		C5		C6	
> 0.5K	1103	0.02%	2778	0.04%	7646	0.12%	11313	0.17%	23193	0.34%	32943	0.48%
> 1.0K	79		278		1006		1544		4011		5822	
> 2.0K	0		1		5		9		77		137	

Over a global number of 6794060 samples.

This table shows that for the worst case (channel 6), the error due to the side lobe is lower than 0.5K for 99.5% of the samples.

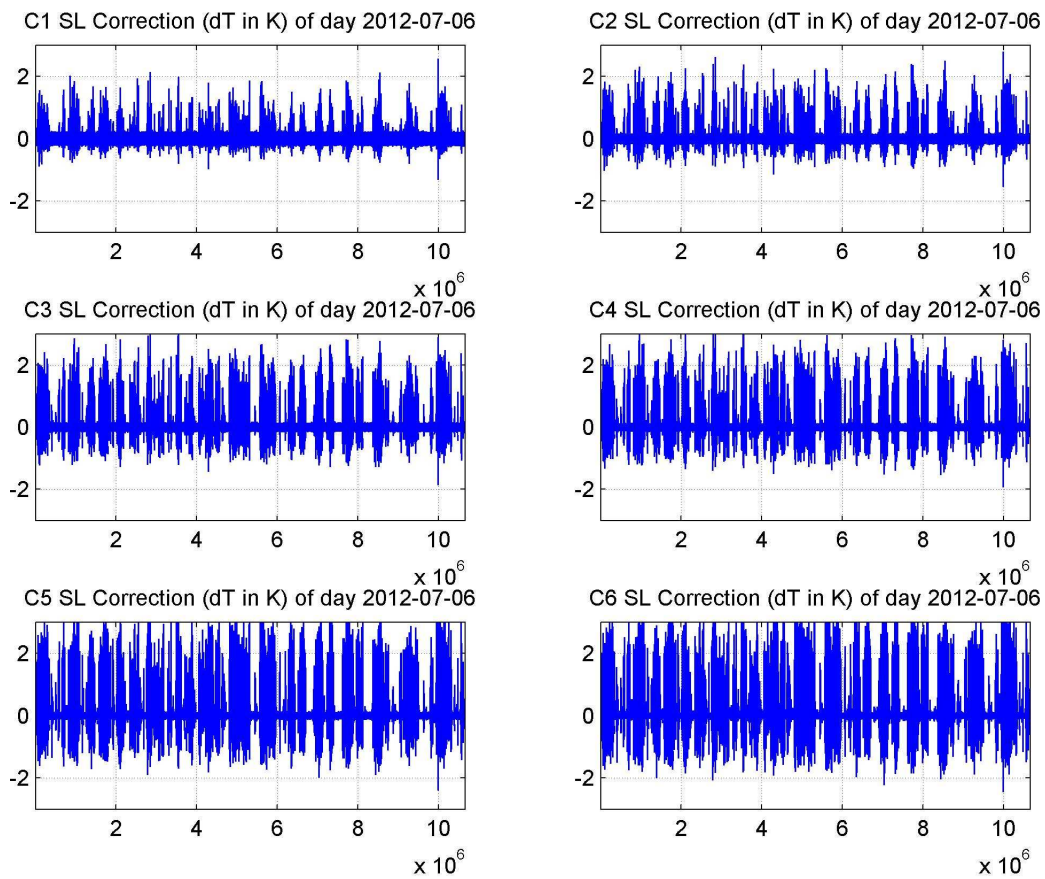
7.2. ANALYSIS OVER 14 ORBITS

This second analysis is done over the 14 orbits of a same day July 6th . Results are shown for all the six channels on following graphs.

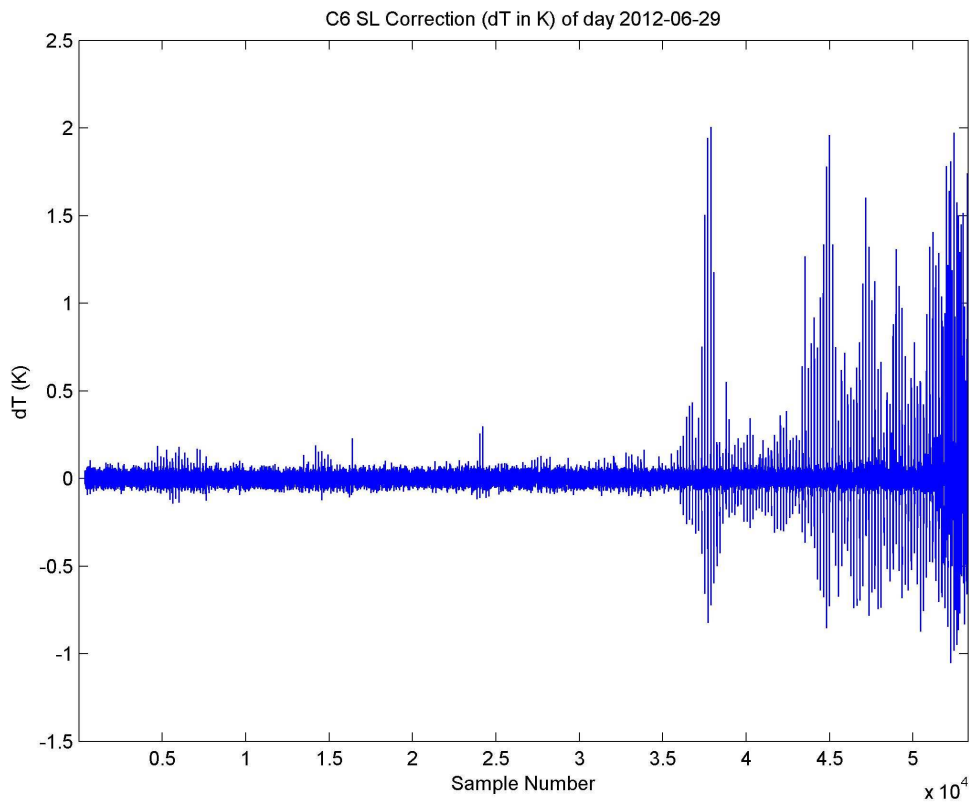
7.2.1. CORRECTION

The following graphs show the variation of the side lobe correction value in a linear representation. The 14 orbits used for this analysis results in $58564 \times 182 = 10658600$ samples.

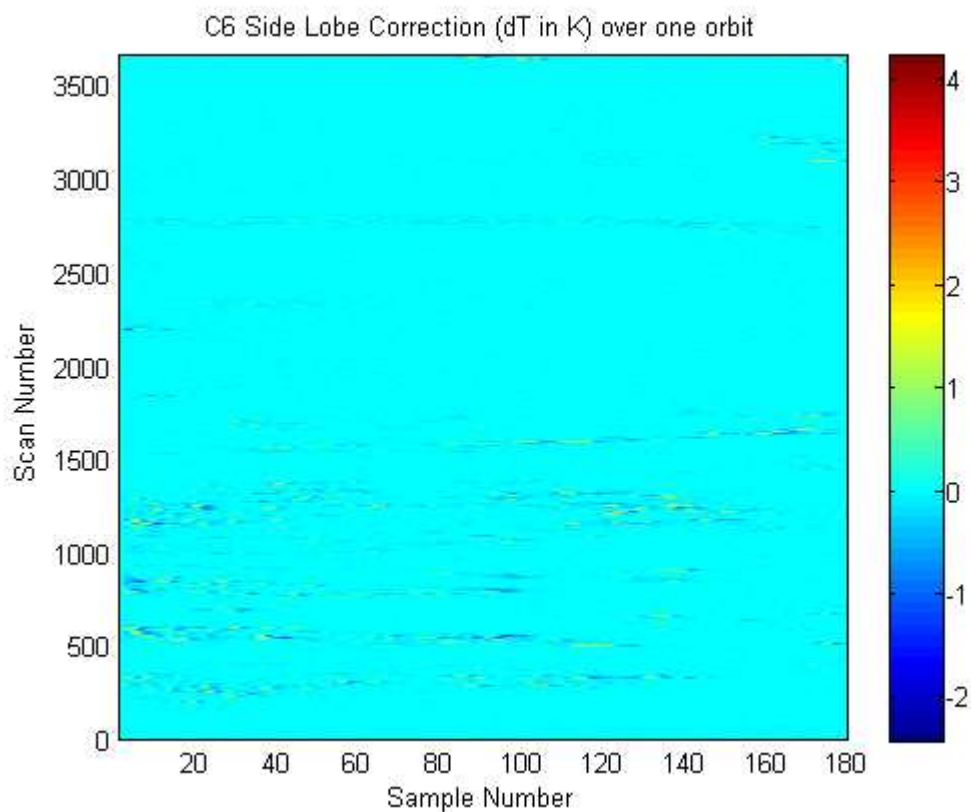
These graphs show that the variations of the side lobe impact follow some temporal cycles which affect all channels. The impact is lower on the channels close to 183.3GHz central frequency.



The scale of the previous figure is a bit tricky to interpret. Then, a zoom of the channel 6 correction due to side lobe is presented hereafter over 300 scans of 182 samples.



The following maps show the side-lobe impact with a 2D representation for the channel 6.



We can see that only a few samples are impacted by the side lobe contamination.

The following table synthesizes the degree of correction to apply due to the side-lobe contamination.

Number of samples	C1		C2		C3		C4		C5		C6	
	> 0.5K	3639	0.03%	9330	0.09%	27369	0.26%	40795	0.38%	78740	0.73%	106422
> 1.0K	465		1587		5279		8129		18598		26707	
> 2.0K	5		42		210		392		1578		2536	

Over a global number of 10658600 samples.

This table shows that for the worst case (channel 6), the error due to the side lobe is lower than 0.5K for 99.0% of the samples.

8. CONCLUSION

The above analysis based on 2 sets of 10 and 14 orbits, demonstrates that the maximum side lobes contribution is observed on channel 6. This sidelobe contribution is higher than 0.5K for less than 0.5% to 1% of the samples. This contribution is lowered to 0.02% for the channel 1.

This could be explained by the fact that roughly less than 1% SAPHIR data have very high gradients compared to surrounding pixels and also by the fact that antenna efficiency for this instrument is quite satisfactory.

Based on these preliminary results, it was decided not to apply any corrections in L1 processing.